

Article

Evaluating the Influence of Different Layouts of Residential Buildings on the Urban Thermal Environment

Yuanyuan Li ¹, Qiang Chen ^{1,*} , Qianhao Cheng ¹, Kangning Li ², Beilei Cao ¹ and Yixiao Huang ¹

¹ School of Geomatics and Urban Spatial Information, Beijing University of Civil Engineering and Architecture, Beijing 102616, China

² Department of Geography, Beijing Normal University, Beijing 100085, China

* Correspondence: chenqiang@bucea.edu.cn; Tel.: +86-152-1098-2439

Abstract: Urban residential building layouts have an impact on air temperature and thermal comfort. Research has shown that poorly designed building layouts can lead to thermal discomfort. Thus, it is crucial to analyze the relationship between residential building layouts and air temperature. We used the ENVI-met 3D microclimate model to simulate six typical residential building layouts and explore the diurnal and seasonal variations in air temperature. In addition, we used the physiological equivalent temperature (PET) as the evaluation index for the thermal comfort of different building layouts. The diurnal results showed that the air temperature of the parallel layout rose faster and fell faster, and these changes were more significant in summer. The results of the air temperature classifications indicated that the frequency of low-air-temperature areas in the parallel layout is approximately 12% smaller than that of the enclosed and semi-enclosed layouts, and the high-air-temperature area frequency is 11% higher than that of the enclosed and semi-enclosed layouts in summer. In winter, the frequency of low-air-temperature areas in the parallel layout is approximately 7% smaller than that of the enclosed and semi-enclosed layouts, and the high-air-temperature area frequency is 5% higher than that of the enclosed and semi-enclosed layouts. In combination with the PET results, we found that the enclosed layout is the optimal configuration. Moreover, in some cases, increased building height and vegetation lead to a reduction in air temperature.

Keywords: residential building layout; ENVI-met; air temperature; urban thermal environment



check for updates

Citation: Li, Y.; Chen, Q.; Cheng, Q.; Li, K.; Cao, B.; Huang, Y. Evaluating the Influence of Different Layouts of Residential Buildings on the Urban Thermal Environment. *Sustainability* **2022**, *14*, 10227. <https://doi.org/10.3390/su141610227>

Academic Editor: Cinzia Buratti

Received: 17 July 2022

Accepted: 15 August 2022

Published: 17 August 2022

Publisher's Note: MDPI stays neutral with regard to jurisdictional claims in published maps and institutional affiliations.



Copyright: © 2022 by the authors. Licensee MDPI, Basel, Switzerland. This article is an open access article distributed under the terms and conditions of the Creative Commons Attribution (CC BY) license (<https://creativecommons.org/licenses/by/4.0/>).

1. Introduction

With the global development of industrialization and the continuous expansion of cities, extreme climates occur frequently. Rapid urbanization has brought a series of problems to human beings; among these, the problem of the urban thermal environment is particularly significant. Massive changes in the material cycle and energy balance associated with urbanization and human-made changes to the Earth's land surface (e.g., the replacement of vegetation with heat-absorbing materials) lead to increased waste heat release [1]. High temperatures sometimes lead to serious health problems, including respiratory problems and cardiovascular or cerebrovascular disease, or even death, especially for seniors. Therefore, there is an urgent need to develop a reasonable plan to alleviate the harm of problems related to the urban thermal environment, especially considering the high-speed development of urban areas. The rapid development of urban layout structures has become more complex, the population density has increased, and the number of buildings has increased. The thermal characteristics of the built environment may produce more serious effects, such as heat waves and the urban heat island (UHI) effect [2].

An urban layout structure is composed of artificial objects, trees, and other natural features, and is highly complex and heterogeneous. The spatial distribution of buildings in a city obviously affects the temporal and spatial variations in solar thermal gain in urban surfaces, and is the main factor affecting urban climate change [3,4]. Residential areas are a

basic part of urban construction areas and an important space for residents to live, so there is a high demand for residential areas that are of high environmental quality. Studies have shown that poorly planned building layouts—the arrangement of buildings that determines ventilation, heat transfer, views, and landscaping—cause discomfort to residents. Buildings can affect microclimates by changing the amount of solar radiation received by the Earth's surface [5,6]. On the one hand, the thermal environment is affected by building layouts, including the aligned parallel layout, the enclosed layout, and the semi-closed layout. On the other hand, the influence of different variables on the thermal environment is also quantified by building height and orientation. Different building layouts have different downwind environments, and buildings play a role in changing the wind profile and reducing the wind speed of the canopy, which may help reduce the sensible heat flux on building surfaces [7,8]. With the increase in building height and density, a large amount of shortwave and longwave radiation is trapped in street canyons; this results in slower heat loss, which in turn leads to the intensification of the urban heat island effect [9,10]. Due to the lack of corresponding scientific theories, more attention is paid to aesthetics and other factors when designing urban buildings, resulting in unreasonable layouts of urban buildings being generated in the urban planning stage [11]. However, the influence of architectural layouts on the thermal environment is too important to be ignored. It is necessary to optimize the spatial layout of buildings and determine whether there is an optimal layout not only to achieve beautiful and pleasant effects, but also to create a more comfortable thermal environment in cities. Most of the above studies take summer climate conditions as their background, and they explore only a few types of building layout models. In the planning and design stages of the different building layouts of urban residential areas, the influence of the thermal environment varies, so the scale of the city and the layout decisions will directly determine the quality of the urban thermal environment [12]. Both livability and the thermal comfort of a reasonable layout are essential for residential buildings, and are also conducive to reducing building energy consumption [13,14].

Acero et al. took Singapore CBD as their research area and designed different scenarios based on determinant layout to explore the influence of street orientation, aspect ratio, and building section height on outdoor thermal comfort in summer, providing sufficient urban parameters for high-rise building development [15]. Srivanit et al. used the climatic conditions of Bangkok as their premise. By changing the canyon orientation and floor area ratio of low-rise townhouses through ENVI-met, a new design standard was proposed to improve the outdoor thermal comfort of residential areas [16]. However, the layout of buildings takes various forms. Therefore, Jiang et al. simulated the layout of typical buildings in summer and found that the thermal comfort of an enclosed layout is better than that of a determinant layout [17]. Taking Ruihai Home in Beijing as their research area, Li Chao et al. explored the microclimate environments of communities living in three building layouts, and found that the enclosed layout performed well and provided people with more comfortable temperature spaces [18]. Wang Weiwu et al. studied the distribution characteristics of the thermal environment in residential areas with three different building layouts in Hangzhou in summer, combining field observations with CFD numerical simulations [19], but this study only explored the summer microclimate environment of three building layouts.

The layout of streets and buildings has been proven to be an important factor affecting the thermal environment, and various studies have investigated the effect of the layout of buildings on thermal comfort. However, few studies have focused on the diurnal dynamic characteristics and seasonal variation of this impact; most previous studies have been conducted in hot dry or hot humid climate areas, based on the climatic conditions in summer [11]. Beijing is a typical mid-latitude northern city with a high degree of development and a diverse building layout. Therefore, we use the microclimate simulation software ENVI-met to construct reliable numerical simulation models, based on typical residential building layouts of Beijing, and estimate the advantages and disadvantages of different typical residential building layouts. We compare the diurnal and seasonal distribution

characteristics of air temperature based on summer and winter conditions. In addition, the physiological equivalent temperature (PET) was used to estimate the thermal comfort of different building layouts. Our findings aim to optimize the thermal environment of human settlements and provide a solid basis for neighborhood reconstruction and future planning.

2. Materials and Methods

2.1. Study Area

As the capital of China, Beijing is affected by a temperate and semihumid continental monsoon climate. It is hot and humid in summer and cold and dry in winter. In normal years, the maximum temperature in summer is as high as 37 °C, and the average temperature in winter is as low as minus 10 °C. Statistics show that, in August 2020, more than half of the 20 weather stations in Beijing broke historical high-temperature records for the same period since the stations were established. Beijing has a high population density, dense buildings, and various architectural layout models. Therefore, we used the climate and building layout of Beijing as a reference to explore the impact of architectural layout on the thermal environment. The geographical location of Beijing is shown in Figure 1a. Figure 1b is the Baidu image of some areas of Beijing. The red dots in the figure represent the geographical locations of each typical residential district explored in this article, and the extracted residential district map is shown in Figure 1c–h.

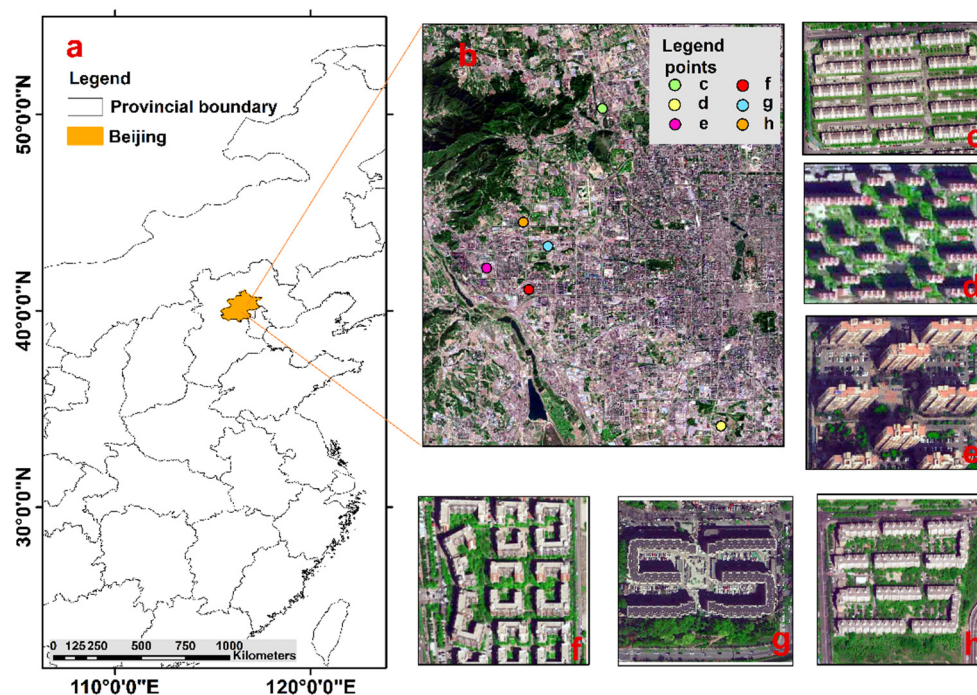


Figure 1. Image of the study area. (a) location of the study sites: Beijing (39° N, 116° E); (b) BaiduMap[®] of the relevant part of Beijing; (c–h) characterization of the typical residential building layouts in this area ((c): 40.01° N, 116.27° E; (d): 39.81° N, 116.37° E; (e): 39.91° N, 116.17° E; (f): 39.92° N, 116.22° E; (g): 39.90° N, 116.21° E; (h): 39.94° N, 116.20° E).

2.2. Methodology

2.2.1. ENVI-Met

In keeping with the purposes of the current research, we used ENVI-met to simulate the surrounding environmental conditions. ENVI-met is a 3D computational dynamics model with a spatial resolution of 0.5–10 m, which is suitable for simulating the interaction between microscale factors that affect the environment. In addition, it obtains and analyzes the exact geographical and climatic location data of the study area. As shown in Figure 2, this model includes the soil model, the one-dimensional boundary model, and the 3D main model area, as well as the inflow boundary and outflow boundary of the 3D main

model area. It has the ability to simulate the main interactions of the atmosphere based on physical laws, such as fluid dynamics and thermodynamics. ENVI-met can be used for microclimate measurement and urban open space analysis, and to measure heat islands and thermal comfort.

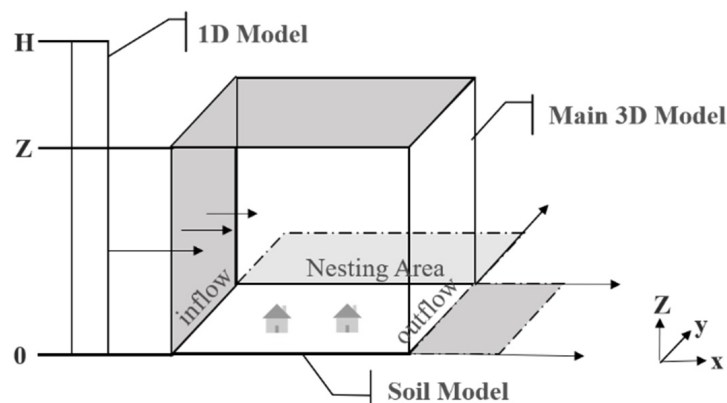


Figure 2. ENVI-met model architecture.

2.2.2. Construction of Simulation Models

We used the forced boundary conditions for turbulence, temperature, and humidity in this paper. The length of each residential building was 60 m, and the width was 15 m. Urban residential buildings were divided into low-rise buildings (1–3 floors), multistory buildings (4–6 floors), medium-high-rise buildings (7–9 floors), and high-rise buildings (above 10 floors), and we chose multistory buildings (6 floors) as the modeling basis. The height of each floor was 3 m, the longitudinal was 24 m, the lateral was 12 m, and the model boundary size was 27 m. The parameter setting of this simulation was also based on the parameters of typical meteorological days in summer in Beijing as the initial input conditions. The simulation area was covered by the mesh of a $100 \times 100 \times 30$ grid, and the grid resolutions were $dx = 4$ m, $dy = 3$ m, and $dz = 3$ m. (dx and dy are horizontal resolutions of x and y , respectively; dz is the resolution of vertical direction z). To ensure the accuracy of the simulation, the simulation of the first 5 h was discarded, and the output of the simulation result was the air temperature at the pedestrian height of 1.5 m above the surface. The geometric settings of the model are listed in Table 1. This study took the climate of Beijing as the background environment, including June, July, and August in summer and December, January, and February in winter. The experiment was carried out based on the meteorological data of a sunny day in summer and winter. The meteorological data in Table 1 are based on data from weather stations in the vicinity of the simulated date.

Table 1. Configuration data used in the ENVI-met simulation.

	Parameter	Values
Initial parameter settings	Total simulation at time/(h)	28
	Number of nested grids	10
	Start simulation at day	Summer: 10 August 2021
Meteorological parameter settings	Start simulation at time	Winter: 7 January 2022
	Min temperature of atmosphere/(°C)	Summer: 23 Winter: −6
	Max temperature of atmosphere/(°C)	Summer: 33 Winter: 6
	Wind speed measured at 10 m/(ms ^{−1})	Summer: 2 Winter: 2
	Wind direction/(°)	Summer: 135 Winter: 257
	Relative humidity at 2 m height/(%)	Summer: 70 Winter: 55
	Specific humidity at model top (2500 m, g/kg)	8

The model constructed in this article represents the layout of major residential areas in Beijing. Six scenarios were designed to explore the impact of the building layout on the thermal environment, as shown in Figure 3: (1) aligned parallel layout, (2) east–west staggered layout, (3) north–south staggered layout, (4) enclosed layout 1, (5) enclosed layout 2, and (6) semi-enclosed layout. Moreover, the aligned parallel layout, east–west staggered layout, and north–south staggered layout were referred to as parallel building layouts. In this article, the enclosed type layouts included enclosed layout 1, enclosed layout 2, and the semi-enclosed layout.

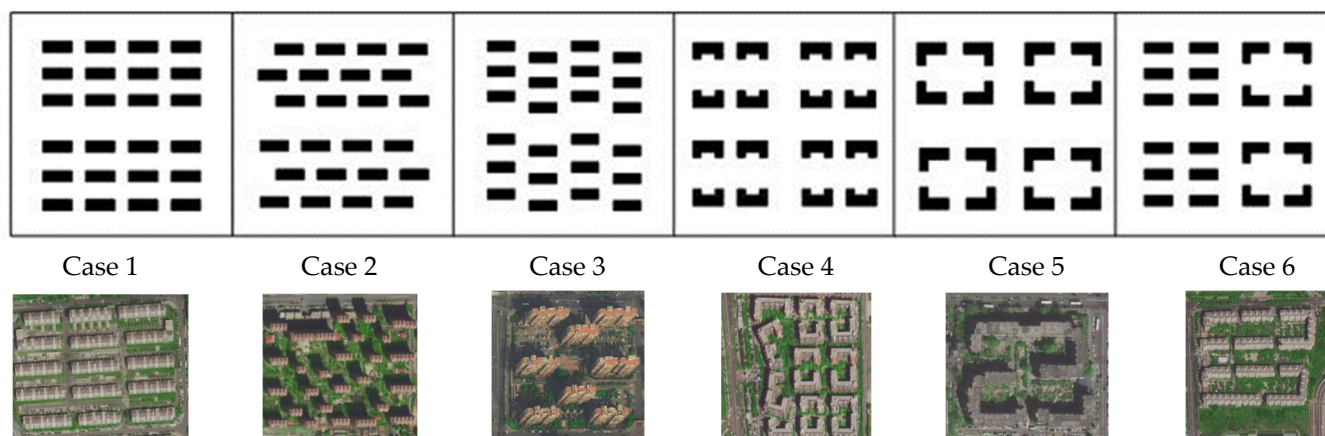


Figure 3. Six typical residential building layout cases in Beijing: (Case 1) aligned parallel layout, (Case 2) east–west staggered layout, (Case 3) north–south staggered layout, (Case 4) enclosed layout 1, (Case 5) enclosed layout 2, and (Case 6) semi-enclosed layout.

2.2.3. Thermal Environment Evaluation Index

According to previous studies, PET and UTCI have relatively complete thermal sensation partitioning [20], and PET has been widely used in many studies on outdoor thermal comfort [21]. PET is defined as the temperature at which the heat balance of the human body is maintained with core and skin temperatures equal to those under the conditions being assessed. This index is based on the Munich Energy-Balance Model for Individuals (MEMI) [22]. It is obtained according to the following formula:

$$S = M \pm W \pm R \pm C \pm K - E - RES, \quad (1)$$

where S = storage heat flows, M = metabolism, W = external work, R = net radiation of the body, C = connective heat flow, K = heat exchange through conduction, E = heat dissipation through evaporation, and RES = heat exchange through respiration (from latent and sensible heat) [23].

Therefore, we used PET as the evaluation index of thermal comfort in this article, and the mean value method to obtain the day and night dynamic change in the mean value of air temperature at every moment. At the same time, the air temperature was statistically analyzed to obtain the area proportion of different air temperature categories, in order to achieve a more intuitive and comprehensive thermal environment assessment system.

The ENVI-met model used the standard human metabolic rate. Other human parameters (age: 35 years; height: 1.75 m; metabolic rate: 86.21 W/m²; clothing: 0.9; weight: 75 kg; and sex: male) were used to calculate PET, which has been widely used to assess outdoor thermal comfort and is considered suitable for its use.

3. Results

We discuss the effects of six different building layout scenarios on the diurnal temperature variation and the thermal environment in summer and winter. The air temperature category area ratio and PET were used to compare the schemes. To exclude the influence of other variables, the article only considered nongreen conditions. The results were based on

the extraction and analysis of day–night data from a horizontal spatial distribution at 1.5 m above the surface.

3.1. The Influence of Building Layouts on Air Temperature and PET in Summer

3.1.1. Variations in Air Temperature under Various Building Layout Scenarios

The air temperature near the surface is one of the important parameters affecting the human somatosensory system. The air temperature at a height of 1.5 m was selected as the output result of the near-surface temperature. By comparing the spatial distributions of air temperatures in different building layouts, as shown in Figure 4, we see that the air temperature in the southeast is higher than that in the northwest: the air temperature in the northwest is approximately 2 °C lower than that in the southeast. The south side of the building is warmer than the north side. These outcomes are related to the wind direction and the shading of the building from the sun's radiation. As seen from the blue area in Figure 3, the low-air-temperature area of the enclosed and semi-enclosed layouts (Cases 4–6) is significantly higher than that of the parallel layout (Cases 1–3), and the low-air-temperature area of the enclosed and semi-enclosed layouts (Cases 4–6) is significantly higher than that of the parallel layout (Cases 1–3).

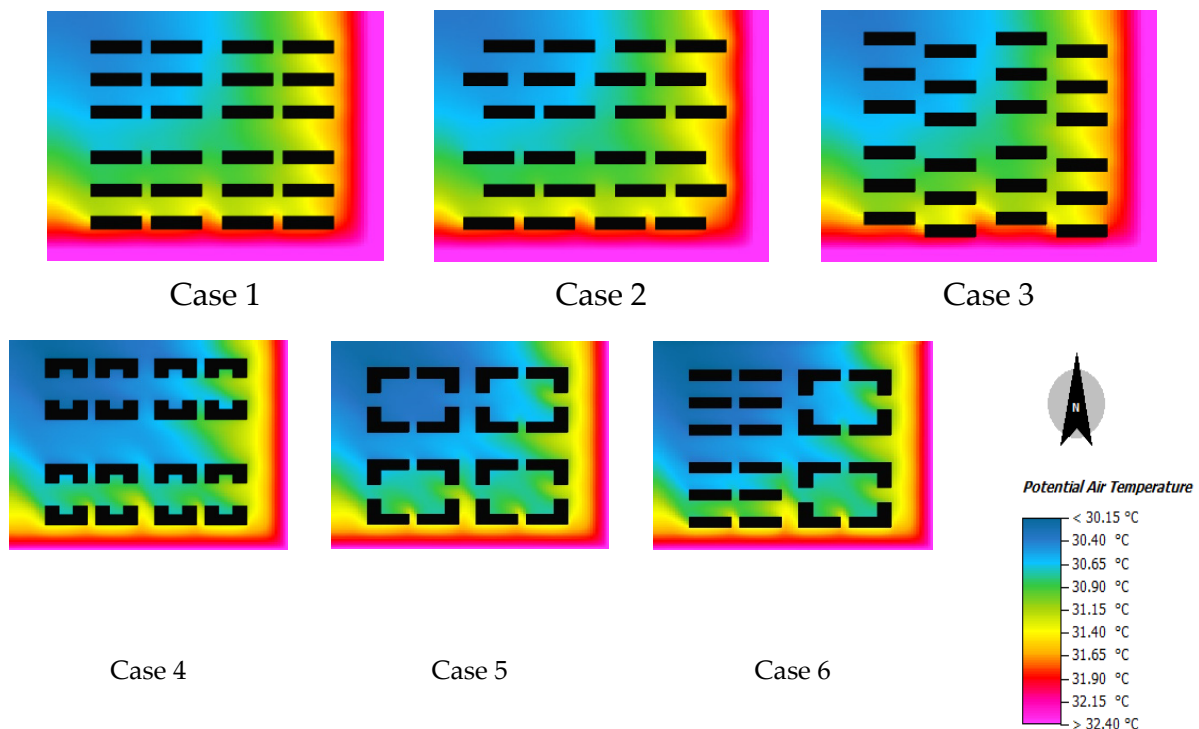


Figure 4. Spatial distribution of pedestrian-level air temperatures at 15:00.

To observe the differences in air temperature between different building layouts more intuitively, the hourly average air temperature results in the daytime (6:00–18:00) and at night (19:00–5:00 the next day) were statistically analyzed, and the results obtained are shown in Figure 5. Before 12:00 noon, the air temperature of the parallel layout (Cases 1–3) is lower than that of the enclosed and semi-enclosed layouts (Cases 4–6); after 12:00 noon, the air temperature exceeds that of Cases 4–6, and then drops to the same air temperature as Cases 4–6 at 22:00. The air temperature of the parallel layout increases faster in the daytime and decreases faster at night. The air temperature of Cases 4–6 shows an obvious fluctuating trend of first rising and then decreasing in the daytime, and first decreasing and then increasing at night. After 22:00 at night, the air temperature exceeds that of Cases 1–3, with a temperature difference of 1.5 °C.

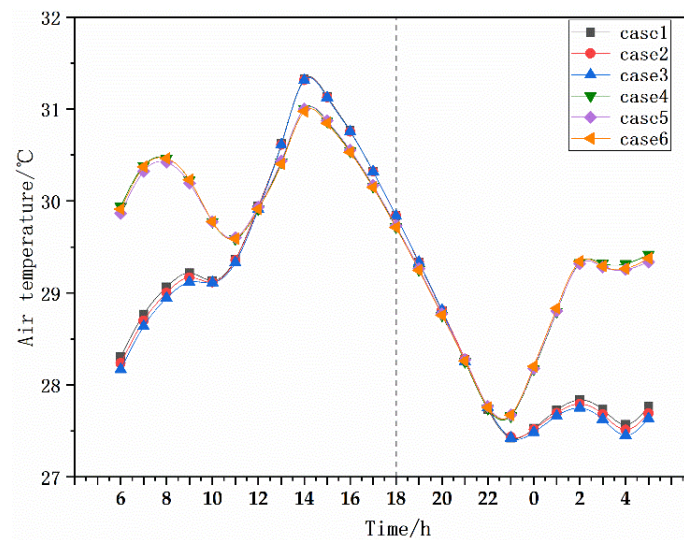


Figure 5. Variation trend of the average air temperature at a height of 1.5 m in different building layouts.

Table 2 shows the thermal spatial differences in the area proportion of different air temperature categories at a height of 1.5 m above the surface. As seen from the table, case 3 has the largest area of high air temperature (35.48%), while case 6 has the smallest area (22.79%). Case 4 has the largest area of low air temperature (24.44%), and case 1 has the smallest area (7.83%). By comparison, the area proportions of low-air-temperature areas in Cases 4–6 are significantly higher than in parallel layouts (Cases 1–3), and the area proportions of high-air-temperature areas in Cases 1–3 are significantly higher than in the enclosed and semi-enclosed layouts in cases 4–6. There is little difference in the proportions of the medium-air-temperature regions. On the whole, in summer, the enclosed and semi-enclosed layouts produce more low-air-temperature areas, smaller high-air-temperature areas, and more comfortable areas.

Table 2. Summary of the relative frequencies of the area occupied by air temperature classifications at 14:00.

Air Temperature Level	Air Temperature (°C)	Relative Frequency (%)					
		Case 1	Case 2	Case 3	Case 4	Case 5	Case 6
High-air-temperature area	$T \geq 31.5$	35.36	34.90	35.48	23.10	23.36	22.79
Medium-air-temperature area	$30.5 \leq T < 31.5$	56.67	56.67	56.01	52.41	53.02	52.81
Low-air-temperature area	$T < 30.5$	7.83	8.38	8.46	24.44	23.58	24.40

3.1.2. PET Layout Effect

Figure 6 displays the horizontal distribution of PET at 1.5 m above the surface at 14:00. In general, PET in the northwest is low and comfortable, while PET in the southeast is high and comfortable. The maximum PET occurred southeast of the area, and the maximum difference in PET for all building layouts reached approximately 3 °C. The PET value on the south side of the building is lower than that on the north side of the building; this may be due to the shadow formed on the north side of the building, which leads to a difference in thermal comfort and indicates that direct solar radiation has an important impact on PET. The PET distribution in Cases 1–3 is relatively consistent, and different staggered modes in the parallel layout have little impact on PET; meanwhile, the distribution of PET in Cases 4–6 differs significantly, indicating that different enclosing modes have a pronounced impact on PET. As seen from the blue area in the northwestern part of the figure, enclosed and semi-enclosed layouts have better thermal comfort.

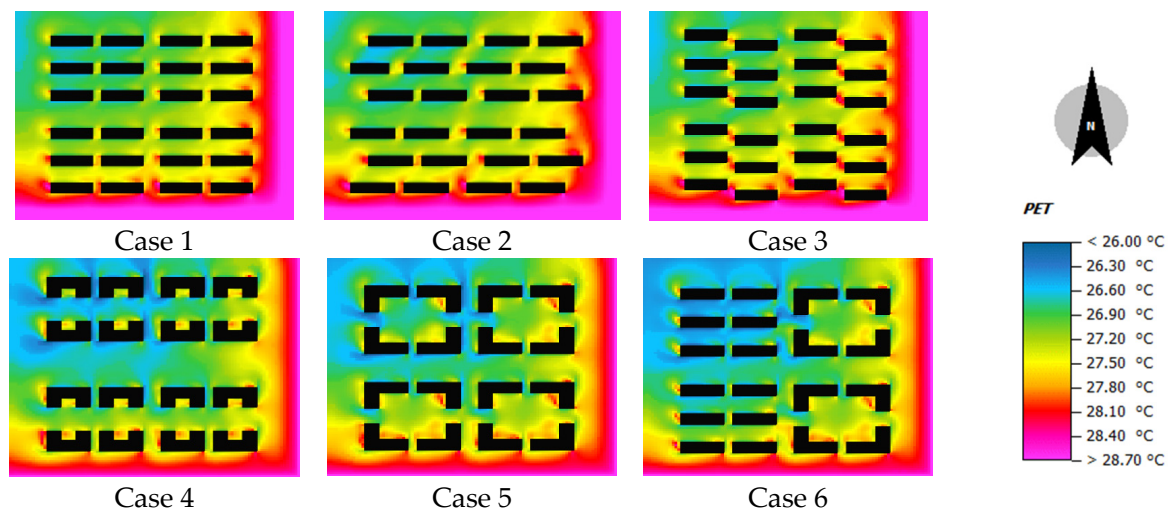


Figure 6. Spatial distribution of PET at a height of 1.5 m in different layouts at 15:00.

Figure 7 shows the mean and maximum distributions of PET for different building layouts at a height of 1.5 m above the surface. In terms of the average PET value, enclosed and semi-enclosed layouts are better than parallel layouts. In parallel layouts, the thermal comfort of case 2 is better, while in enclosed and semi-enclosed layouts, the thermal comfort of case 6 is better. The maximum and minimum PET values of the parallel layout are higher than those of the enclosed layout and semi-enclosed layout.

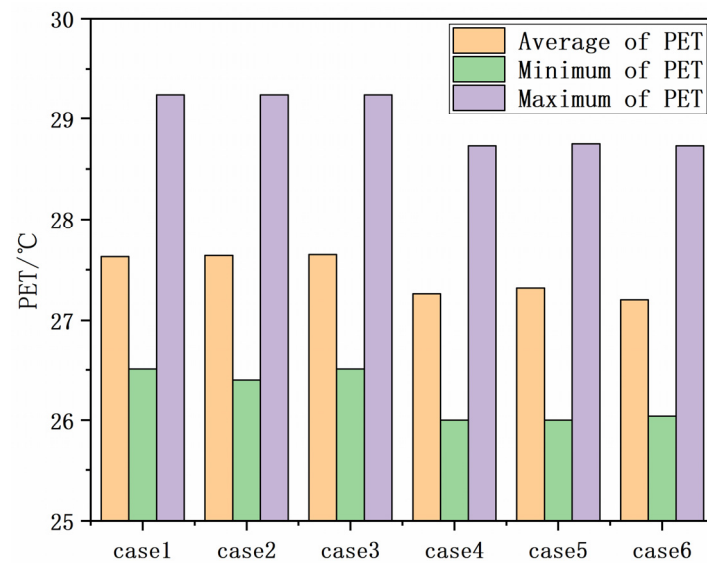


Figure 7. PET values at a height of 1.5 m in different building layouts at 14:00.

3.2. The Influence of Building Layout on Air Temperature and PET in Winter

3.2.1. Variations in Air Temperature under Various Building Arrangement Scenarios

Figure 8 shows the spatial distribution results of near-surface air temperature at 1.5 m above the surface in winter. In an obvious difference from summer, the high-air-temperature area is mainly distributed in the southwest in winter, while the low-air-temperature area is mainly distributed in the east and north. The wind direction has an influence on the distribution of air temperatures. It can be seen from the figure that the temperature difference between the low-air-temperature and high-air-temperature areas is as high as 2.7 °C. Meanwhile, it can be observed that enclosed and semi-enclosed layouts (Cases 4–6) have a greater area of low-air-temperature areas than that of parallel layouts (Cases 1–3).

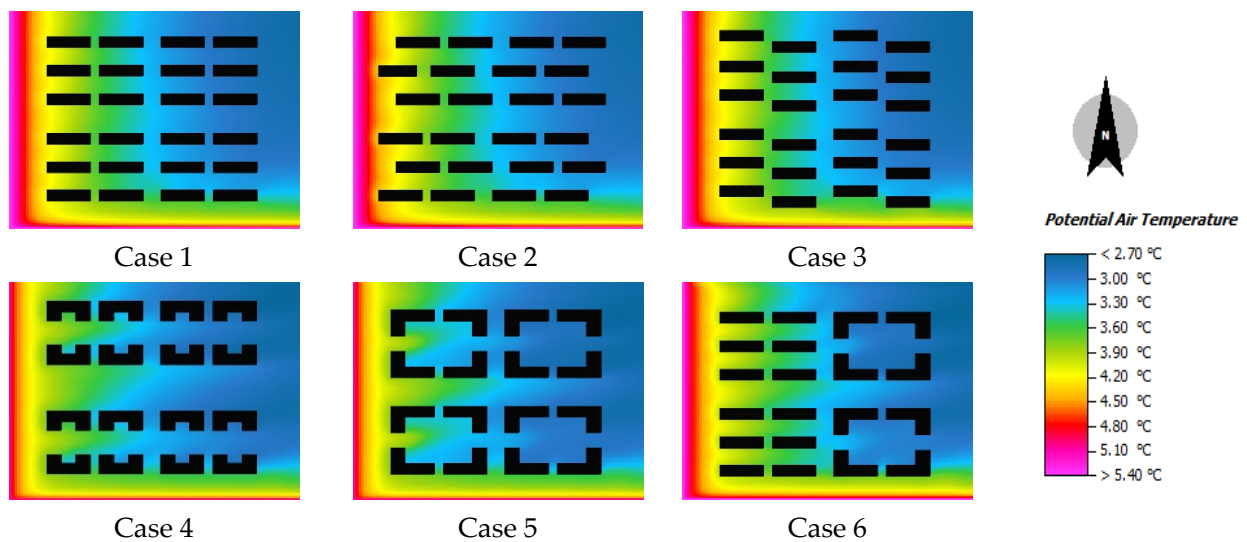


Figure 8. Spatial distribution of pedestrian-level air temperature at 15:00.

Figure 9 shows the increasing and decreasing trends of the day and night mean air temperatures in winter. First, the air temperature variation trends of Cases 1–3 and Cases 4–6 are consistent in the daytime, showing that temperatures first rise and then decrease overall. Before 13:00, the air temperature of Cases 4–6 is always higher than that of Cases 1–3. After 13:00, the air temperature of cases 1–3 begins to be higher than that of Cases 4–6. The air temperature reached the maximum value at 14:00 and then began to decline. After 17:00, the air temperature of Cases 1–3 becomes lower than that of Cases 4–6. At night, the air temperature of different building layouts always shows a decreasing trend before 4:00, and the air temperature of Cases 4–6 is always higher than that of Cases 1–3. The difference is that the range of the change in air temperature in Cases 4–6 is gentler between 0:00–4:00, and the air temperature begins to rise after 4:00.

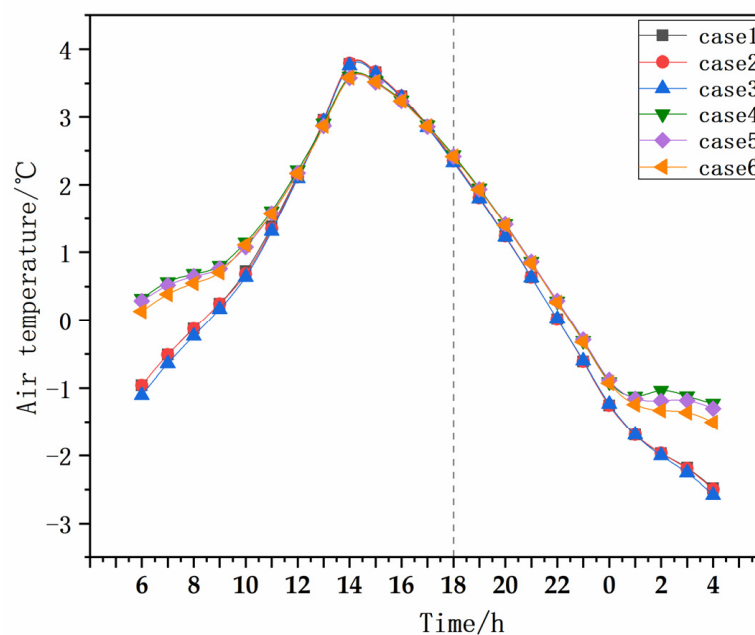


Figure 9. Variation trend of average air temperature at a height of 1.5 m in different building layouts.

Table 3 shows the relative frequencies of areas occupying different air temperature categories at 1.5 m above the surface at 14:00 in winter. For the high-air-temperature area, case 2 has the largest area (13.15%), while case 6 has the smallest area (7.12%). For the low-

air temperature region, case 5 has the largest area (66.55%), and case 2 has the smallest area (57.56%). As a whole, the parallel layout (Cases 1–3) produces more high-air-temperature areas than the semi-enclosed layout (Cases 4–6) and fewer low-air-temperature areas than the semi-enclosed layout. Although the parallel layout has a large range of temperature variation, it provides more high-air-temperature areas in winter; in contrast, the enclosed and semi-enclosed layouts have a small temperature variation range. However, the lower height of the sun in winter produces more shadowy areas than in summer, resulting in a larger area of low air temperature.

Table 3. Summary of the relative frequencies of the areas occupied by air temperature classifications at 14:00.

Air Temperature Level	Air Temperature (°C)	Relative Frequency (%)					
		Case 1	Case 2	Case 3	Case 4	Case 5	Case 6
High-air-temperature area	$T \geq 4.8$	12.84	13.15	13.01	7.22	7.21	7.12
Medium-air-temperature area	$3.8 \leq T < 4.8$	29.22	29.24	27.11	27.85	26.20	28.28
Low-air-temperature area	$T < 3.8$	57.90	57.56	59.83	64.88	64.55	64.55

3.2.2. PET Layout Effect

Figure 10 shows the spatial distribution of PET at 1.5 m above the surface at 14:00 in winter. Overall, the PET values were lower in the southwest and higher in the west and near the buildings. The wind direction is northwest, and the PET value on the leeward side of the building is higher than that on the windward side of the building due to the building blocking the wind, resulting in better comfort. From the pink and red areas in the figure, it can be seen that the thermal comfort of the enclosed and semi-enclosed layouts (Cases 4–6) is better than that of the parallel layouts (Cases 1–3).

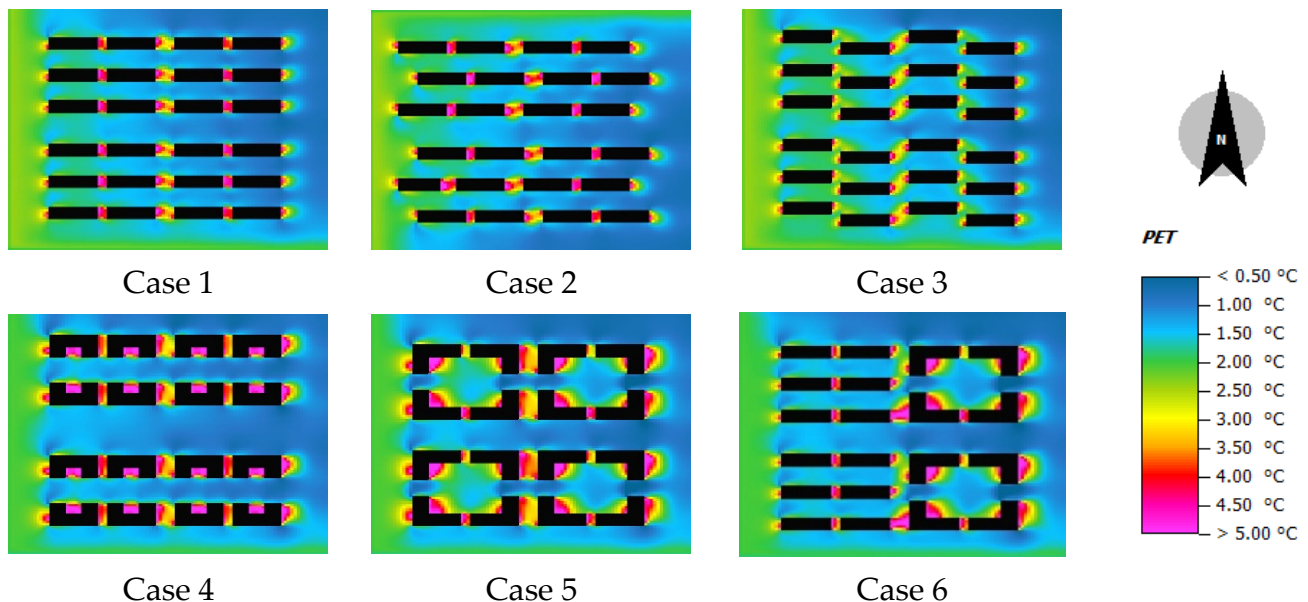


Figure 10. Spatial distribution of PET at a height of 1.5 m in different layouts at 15:00.

Figure 11 shows the mean, maximum, and minimum values of PET at 1.5 m above the surface for different building layouts at 14:00. It can be seen from the figure that the maximum PET value appeared in case 2, while the mean PET value did not change significantly. The minimum PET value appeared in case 6. In addition, it can be seen that the minimum PET value of Cases 1–3 is significantly higher than that of Cases 4–6.

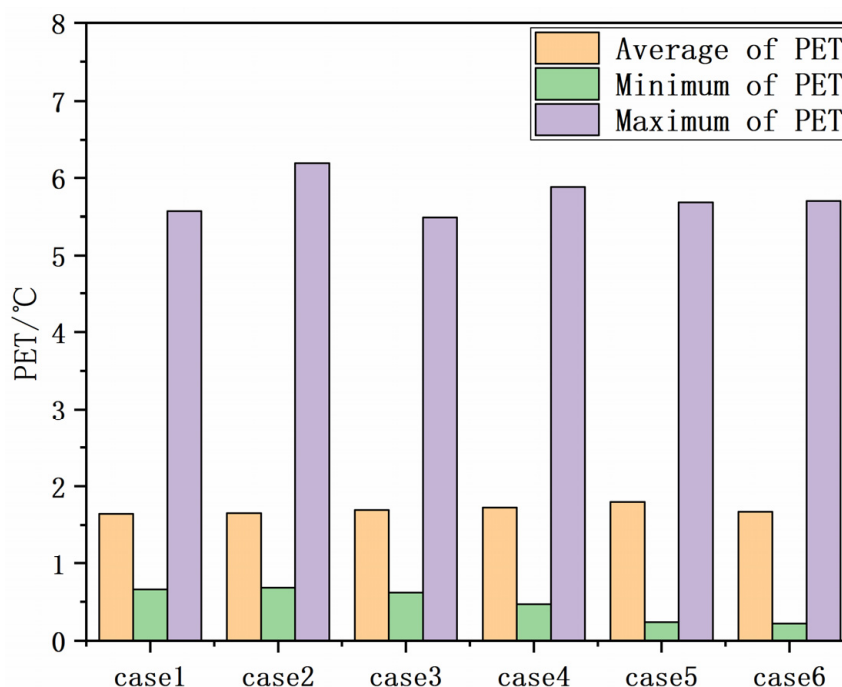


Figure 11. PET values at a height of 1.5 m in different building layouts at 14:00. AT: air temperature.

4. Discussion

In addition to the different building arrangements, building height and vegetation affect the air temperature distribution in architectural layouts. Using a remote sensing method, Wang and others found that an increase in building height will produce a cooling effect [24]. In addition, some studies have reported that adding a single building construction area and increasing the number of floors can increase the shading effect [25]. According to the above results, case 4 performs better in summer, providing more low-temperature areas. Therefore, it makes most sense to discuss case 4, so we selected case 4 as the main scenario. With the climatic conditions in summer and winter as the background, the influence of building height on air temperature was explored by changing the building height to 9 m, 18 m, and 36 m. The influence of vegetation on air temperature was also explored by adding vegetation in case 4 as the principal scenario.

4.1. The Impact of Building Height on Air Temperature

The building scene simulated in the previous experiment was a multistory residential area (4–6 floors), and the building height was set at 18 m. Therefore, using case 4 (which performed well in summer) as the principal scenario, we explored the influence of building height on air temperature by changing the building height to 9 m, 18 m, and 36 m, with the climatic conditions in summer and winter as the background. Figure 12a shows the classification of air temperatures in summer based on the air temperature at 1.5 m above the surface at 14:00 in case 4. It can be seen that, with the increase in building height, the proportion of the low-air-temperature area increases from 18.21% at 9 m to 28.52% at 36 m. Similarly, with increasing height, the proportion of the area with a high air temperature decreases, with a difference of nearly 3.64%. Figure 12b shows the classification of air temperature in winter based on the air temperature at 1.5 m above the surface at 14:00 in case 4. It can be seen that there is no significant difference in high-air-temperature areas. With the increasing height of the building, the area proportion of the medium-air-temperature region increases, while that of the low-air-temperature region tends to decline.

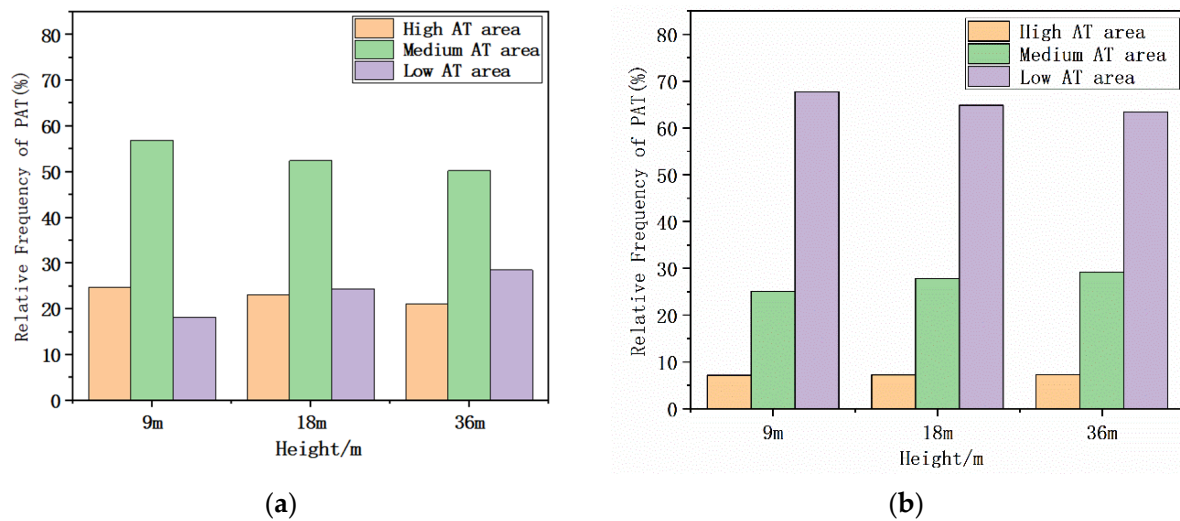


Figure 12. Area ratio for air temperature categories of different building heights in case 4 at 14:00. (a) summer, (b) winter.

4.2. The Impact of Vegetation Cover on Air Temperature in Building Layouts

The optimization of the building layout is an important aspect of sustainable urban development. In the previous height experiment, it was found that the higher the building, the more shadow areas are provided in summer. Vegetation regulates solar radiation, reduces reradiation from impervious surfaces, and provides a potential cooling effect through evapotranspiration [26]. Therefore, continuing to use case 4 as our basis, we discuss the influence of vegetation in building layouts on the thermal environment.

It can clearly be seen from Figure 13 that the proportion of the area with a high air temperature in the scenario without vegetation coverage (10.83%) is greater than that in the scenario with vegetation (23.1%), with the proportion difference being approximately 10%. The proportion of the area (24.44%) in the low-air-temperature region without vegetation was smaller than that in the low-air temperature region with vegetation (65%), indicating that vegetation had a cooling effect on air temperature.

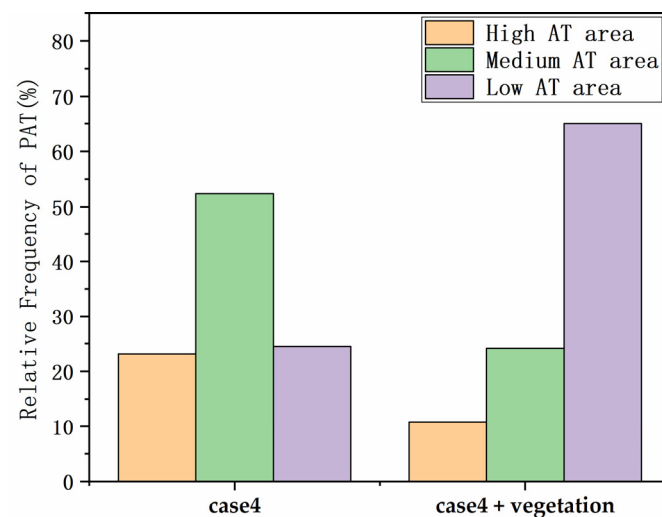


Figure 13. The area ratio of air temperature categories in case 4, at 14:00, for areas with vegetation and without vegetation.

5. Conclusions

In this paper, we adopted the numerical simulation method to simulate the thermal environmental characteristics of six typical residential building layouts using ENVI-met.

Our findings showed that the thermal comfort of enclosed and semi-enclosed layouts is better than that of parallel layouts; this result has also been proven by previous research studies [17]. However, previous studies mainly discussed the influence of building layouts on the thermal environment in summer, and little consideration has been given to seasonal effects; as such, we analyzed how the influence of building layouts on air temperature differed between summer and winter.

In summer, according to the average air temperature value at 1.5 m above the surface, and the proportion of the area characterized by different air temperature grades, the maximum average air temperature value of the parallel layout was higher than that of the enclosed and semi-enclosed layouts. Additionally, the low-temperature area generated by the parallel layout was smaller than that of the enclosed and semi-enclosed layouts. Thus, the thermal environment of the enclosed layout is superior to that of the parallel layout, which is consistent with Jiang's research on building layouts in high-temperature and high-humidity areas [17]. However, in winter, the L-shaped and U-shaped buildings with enclosed and semi-enclosed layouts have more shaded areas and a higher proportion of low-temperature areas compared with the determinant layout, due to the decrease in the solar altitude angle. The high-temperature area of the determinant layout is larger than that of the closed and semi-enclosed layouts; thus, the parallel layout is superior to the closed and semi-closed layouts.

From the perspective of the PET, the regional thermal comfort difference mainly arises because the PET is greatly affected by solar radiation, and building shadows can effectively improve thermal comfort [27–29]. Enclosed and semi-enclosed layouts had lower PET values in summer than parallel layouts, and enclosed and semi-enclosed layouts had higher PET values in winter than parallel layouts. On the whole, the thermal comfort of enclosed and semi-enclosed layouts is better than that of parallel layouts. According to these results, we find that enclosed and semi-enclosed layouts are more suitable for northern cities such as Beijing.

In this research, we only investigated the horizontal distribution of air temperature and PET at 1.5 m above the surface, and did not consider the distribution at different heights. Moreover, the ratio of the height of buildings to their distance from each other (H/W) was not considered. Therefore, future research should consider the H/W ratio and optimize the model to make the results more robust.

Author Contributions: Conceptualization, Q.C. (Qiang Chen); methodology, Y.L.; software, Y.L.; validation, Q.C. (Qiang Chen); formal analysis, Q.C. (Qiang Chen); investigation, Y.L.; data curation, Y.L.; writing—original draft preparation, Y.L. (Yuanyuan Li); writing—review and editing, Q.C. (Qiang Chen), Y.L., Q.C. (Qianhao Cheng), K.L., B.C., Y.H.; visualization, Y.L.; supervision, Q.C. (Qian Cheng), K.L., B.C., Y.H.; project administration, Q.C. (Qiang Chen); funding acquisition, Q.C. (Qiang Chen). All authors have read and agreed to the published version of the manuscript.

Funding: This research was supported by the National Natural Science Foundation (NSFC) of China (41930650) and the General project of Beijing Municipal Science and Technology Commission (KM201910016006).

Institutional Review Board Statement: Not applicable.

Informed Consent Statement: Not applicable.

Data Availability Statement: The data that support the findings of this study are available from the author upon reasonable request.

Acknowledgments: The authors would like to thank Yunhao Chen for his effective suggestions on this paper, and the anonymous reviewers for their constructive comments on the earlier version of the manuscript.

Conflicts of Interest: The authors declare no conflict of interest.

References

1. Shi, X.; Yang, J. A material flow-based approach for diagnosing urban ecosystem health. *J. Clean. Prod.* **2014**, *64*, 437–446. [[CrossRef](#)]
2. Hondula, D.M.; Barnett, A.G. Heat-related morbidity in Brisbane, Australia: Spatial variation and area-level predictors. *Environ. Health Perspect.* **2014**, *122*, 831–836. [[CrossRef](#)]
3. Yu, B.; Liu, H.; Wu, J.; Lin, W.-M. Investigating impacts of urban morphology on spatio-temporal variations of solar radiation with airborne LIDAR data and a solar flux model: A case study of downtown Houston. *Int. J. Remote Sens.* **2009**, *30*, 4359–4385. [[CrossRef](#)]
4. Wang, B.; Koh, W.S.; Liu, H.; Yik, J.; Bui, V.P. Simulation and validation of solar heat gain in real urban environments. *Build. Environ.* **2017**, *123*, 261–276. [[CrossRef](#)]
5. Wu, Z.; Dou, P.; Chen, L. Comparative and combinative cooling effects of different spatial arrangements of buildings and trees on microclimate. *Sustain. Cities Soc.* **2019**, *51*, 101711. [[CrossRef](#)]
6. Wollmann, C.A.; Hoppe, I.L.; Gobo, J.P.A.; Simioni, J.P.D.; Costa, I.T.; Baratto, J.; Shooshtarian, S. Thermo-hygrometric variability on waterfronts in negative radiation balance: A case study of balneário Camboriú/SC, Brazil. *Atmosphere* **2021**, *12*, 1453. [[CrossRef](#)]
7. Britter, R.; Hanna, S. Flow and dispersion in urban areas. *Annu. Rev. Fluid Mech.* **2003**, *35*, 469–496. [[CrossRef](#)]
8. Hang, J.; Sandberg, M.; Li, Y. Effect of urban morphology on wind condition in idealized city models. *Atmos. Environ.* **2009**, *43*, 869–878. [[CrossRef](#)]
9. Gago, E.J.; Roldan, J.; Pacheco-Torres, R.; Ordóñez, J. The city and urban heat islands: A review of strategies to mitigate adverse effects. *Renew. Sustain. Energy Rev.* **2013**, *25*, 749–758. [[CrossRef](#)]
10. Zhang, J. Study on the Influence of Underlying Surface Properties on the Thermal Environment of Lhasa Street and Its Design Strategy. Master's Thesis, Southwest Jiaotong University, Chengdu, China, 2018.
11. Mk, A.; Mss, B. The effect of height and orientation of buildings on thermal comfort. *Sustain. Cities Soc.* **2022**, *79*, 103720.
12. Diao, Z. Influence of Block Scale Building Layout on Block Building Energy Consumption in Harbin Old City. Master's Thesis, Harbin Engineering University, Harbin, China, 2018.
13. Zhao, Q.; Sailor, D.J.; Wentz, E.A. Impact of tree locations and arrangements on outdoor microclimates and human thermal comfort in an urban residential environment. *Urban For. Urban Green.* **2018**, *32*, 81–91. [[CrossRef](#)]
14. Chan, A. Effect of adjacent shading on the thermal performance of residential buildings in a subtropical region. *Appl. Energy* **2012**, *92*, 516–522. [[CrossRef](#)]
15. Acero, J.A.; Koh, E.J.; Ruefenacht, L.A.; Norford, L.K. Modelling the influence of high-rise urban geometry on outdoor thermal comfort in Singapore. *Urban Clim.* **2021**, *36*, 100775. [[CrossRef](#)]
16. Srivani, M.; Jareemit, D. Modeling the influences of layouts of residential townhouses and tree-planting patterns on outdoor thermal comfort in Bangkok suburb. *J. Build. Eng.* **2020**, *30*, 101262. [[CrossRef](#)]
17. Jiang, Y.; Wu, C.; Teng, M. Impact of Residential Building Layouts on Microclimate in a High Temperature and High Humidity Region. *Sustainability* **2020**, *12*, 1046. [[CrossRef](#)]
18. Li, C.; Yang, X. Influence of community building arrangement on microclimate environment based on numerical simulation. *Urban Build.* **2021**, *18*, 56–59.
19. Wang, W.; Yang, H.; Shao, Y.; Tang, S. Simulation of three-dimensional distribution characteristics of outdoor thermal environment in urban residential areas: A case study of Hangzhou. *J. Zhejiang Univ. Eng.* **2013**, *47*, 1178–1185.
20. Zhang, W.; Hu, Z.; Ding, W. Research progress of outdoor thermal comfort index. *J. Environ. Health* **2015**, *32*, 836–841.
21. Guo, S.; Yang, F.; Jiang, Z. Thermal environmental effects of vertical greening and building layout in open residential neighbourhood design: A case study in Shanghai. *Archit. Sci. Rev.* **2022**, *65*, 72–88. [[CrossRef](#)]
22. Hppe, P.R. The physiological equivalent temperature—A universal index for the biometeorological assessment of the thermal environment. *Int. J. Biometeorol.* **1999**, *43*, 71–75. [[CrossRef](#)]
23. Jamei, E.; Rajagopalan, P. Urban development and pedestrian thermal comfort in Melbourne. *Sol. Energy* **2017**, *144*, 681–698. [[CrossRef](#)]
24. Wang, M.; Xu, H. The impact of building height on urban thermal environment in summer: A case study of Chinese megacities. *PLoS ONE* **2021**, *16*, e0247786. [[CrossRef](#)] [[PubMed](#)]
25. Ignatius, M.; Wong, N.H.; Jusuf, S.K. Urban microclimate analysis with consideration of local ambient temperature, external heat gain, urban ventilation, and outdoor thermal comfort in the tropics. *Sustain. Cities Soc.* **2015**, *19*, 121–135. [[CrossRef](#)]
26. Wilmers, F. Effects of vegetation on urban climate and buildings. *Energy Build.* **1990**, *15*, 507–514. [[CrossRef](#)]
27. Zheng, Y.; Yin, J.; Wu, R.; Ye, D. Applicability of universal thermal climate index to thermal comfort forecast. *J. Appl. Meteorol.* **2010**, *21*, 709–715.
28. Park, S.; Tuller, S.E.; Jo, M. Application of Universal Thermal Climate Index (UTCI) for microclimatic analysis in urban thermal environments. *Landsc. Urban Plan.* **2014**, *125*, 146–155. [[CrossRef](#)]
29. Bröde, P.; Krüger, E.L.; Rossi, F.A.; Fiala, D. Predicting urban outdoor thermal comfort by the Universal Thermal Climate Index UTCI—A case study in Southern Brazil. *Int. J. Biometeorol.* **2012**, *56*, 471–480. [[CrossRef](#)]